

Supporting Information (SI) for:

Facile *In-Situ* Synthesis of Crystalline VOOH-Coated VS₂ Microflowers with Superior Sodium Storage Performance

Wenbin Li,^a Jianfeng Huang,^{*a} Liangliang Feng,^a Liyun Cao,^a Yongqiang Feng,^a Haijing Wang,^a Jiayin Li,^a Chunyan Yao,^b

^a School of Materials Science & Engineering, Shaanxi University of Science and Technology,
Xi'an Shaanxi 710021, P.R. China

^b Culture and Communication School, Shaanxi University of Science and Technology, Xi'an
Shaanxi 710021, P.R. China

*E-mail: huangjf@sust.edu.cn

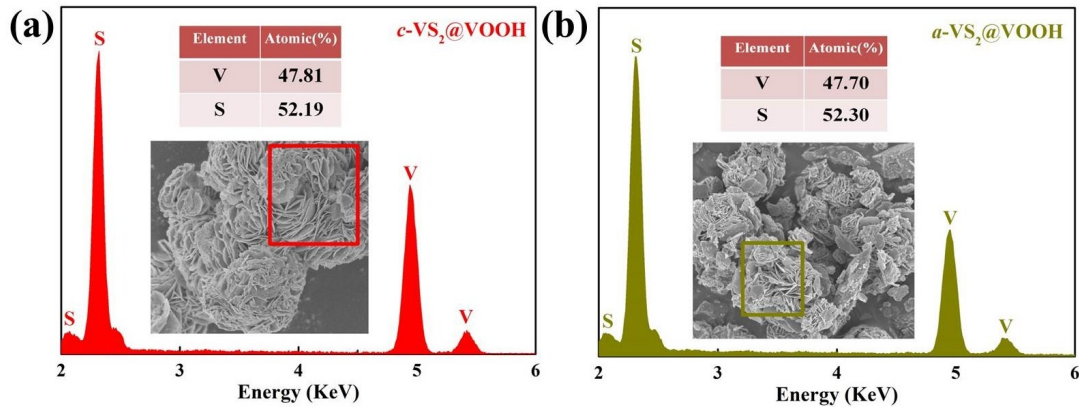


Fig. S1 EDS spectra of (a) *c*-VS₂@VOOH microflowers and (b) *a*-VS₂@VOOH microflowers obtained by SEM-EDS.

The weight percent of VOOH in VS₂@VOOH is calculated by the following equation:

$$W_{\text{VOOH}} = \frac{(A_v - A_s/2) \times M_{\text{VOOH}}}{(A_v - A_s/2) \times M_{\text{VOOH}} + A_s/2 \times M_{\text{VS}_2}} \times 100\%$$

where W_{VOOH} is the weight percent of VOOH in VS₂@VOOH. A_v and A_s are the atomic percent of V and S, respectively. M_{VOOH} and M_{VS_2} are the molar mass of VOOH and VS₂, respectively.

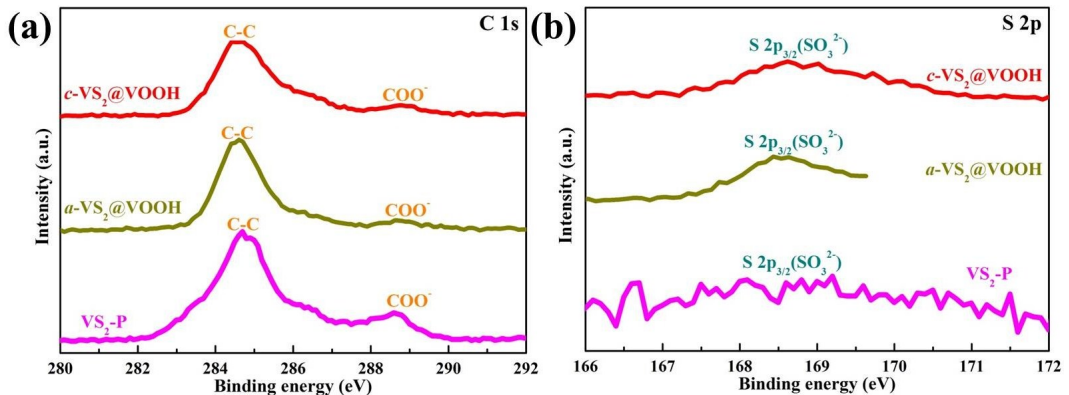


Fig. S2 High resolution (a) C 1s and (b) S 2p XPS spectra for *c*-VS₂@VOOH, *a*-VS₂@VOOH and VS₂-P.

The binding energy at ~ 288.9 eV in Fig. S2(a) further shows the existence of COO⁻,² and the value of ~ 168.8 eV in Fig. S2(b) is consistent with the reported value for S⁴⁺ in S 2p spectral region^{3,4}, further declaring the existence of SO₃²⁻ groups.

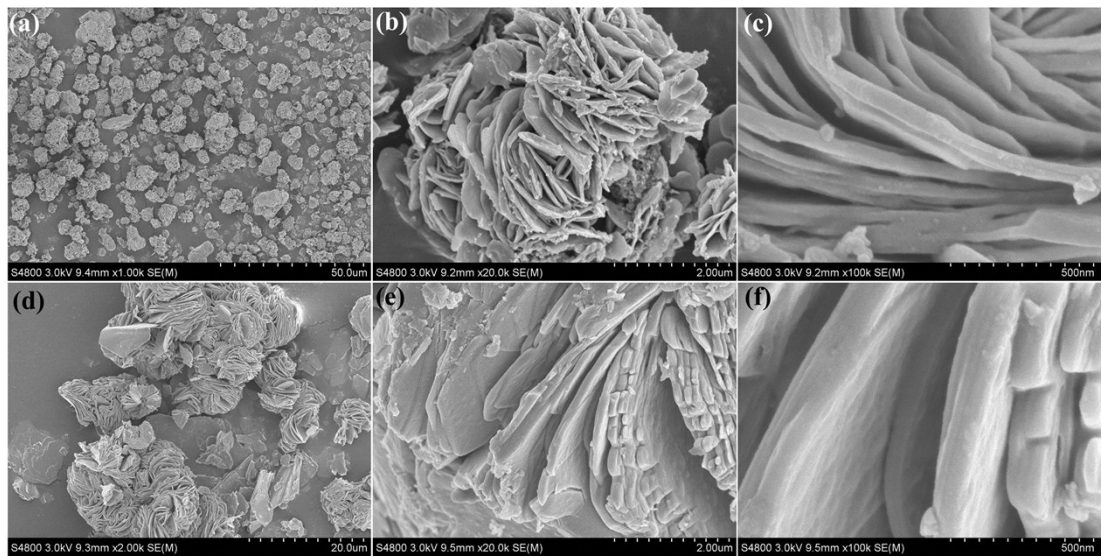


Fig. S3 SEM images of (a ~ c) $a\text{-VS}_2@\text{VOOH}$ and (d ~ f) $\text{VS}_2\text{-P}$.

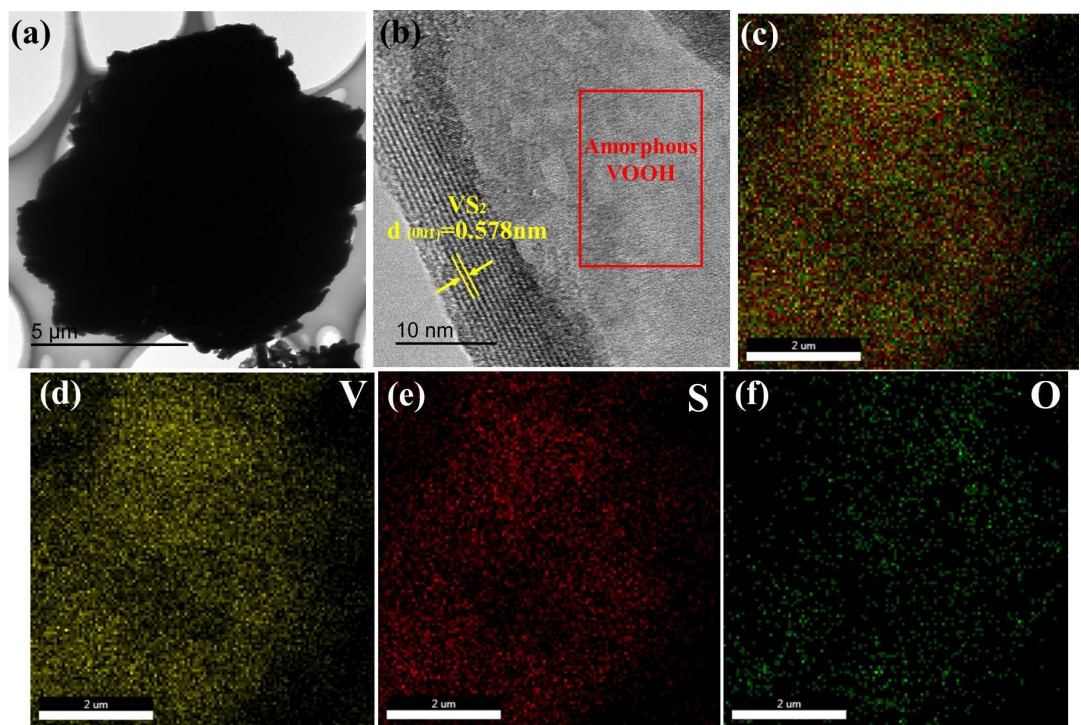


Fig. S4 (a) Low-magnification TEM image, (b) HRTEM image and (c ~ f) elemental mapping images of $a\text{-VS}_2@\text{VOOH}$ microflower.

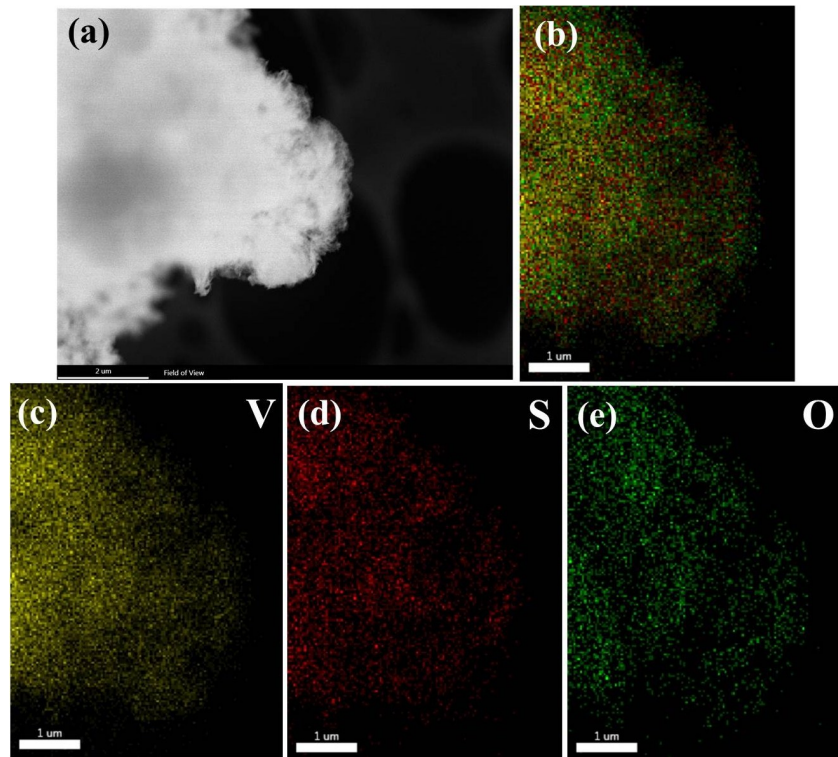


Fig. S5 (a) STEM image and (b ~ e) the corresponding elemental mapping images of *c*-VS₂@VOOH microflower.

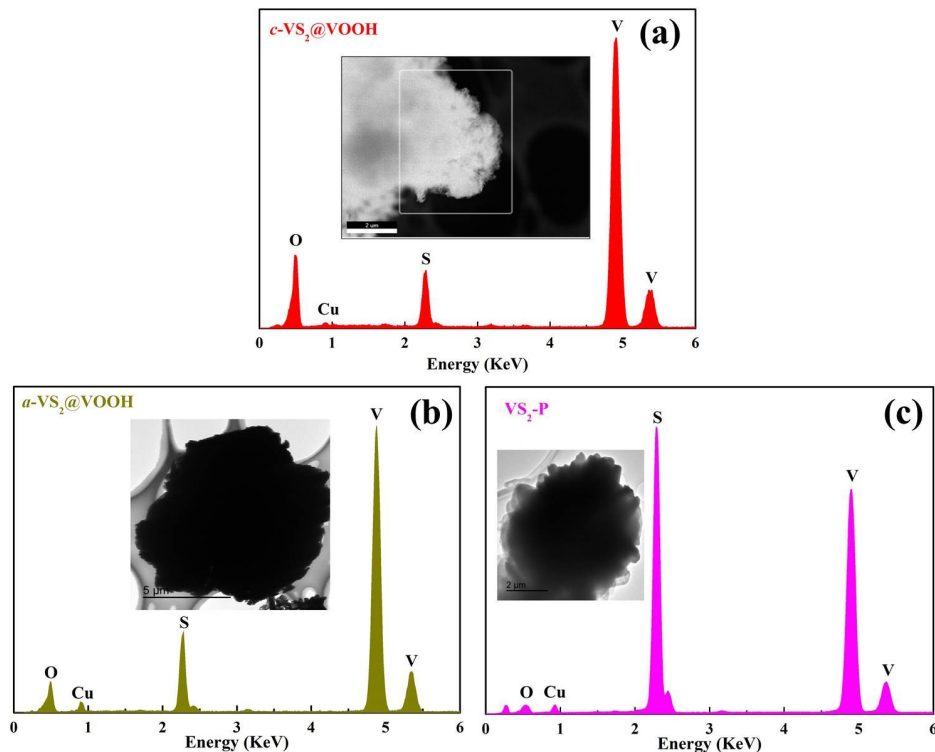


Fig. S6 EDS spectra of the map scanning corresponding to the low-magnification TEM images of (a) *c*-VS₂@VOOH, (b) *a*-VS₂@VOOH and (c) VS₂-P, which were obtained by STEM-EDS with the detection depth of ~ 10 nm.

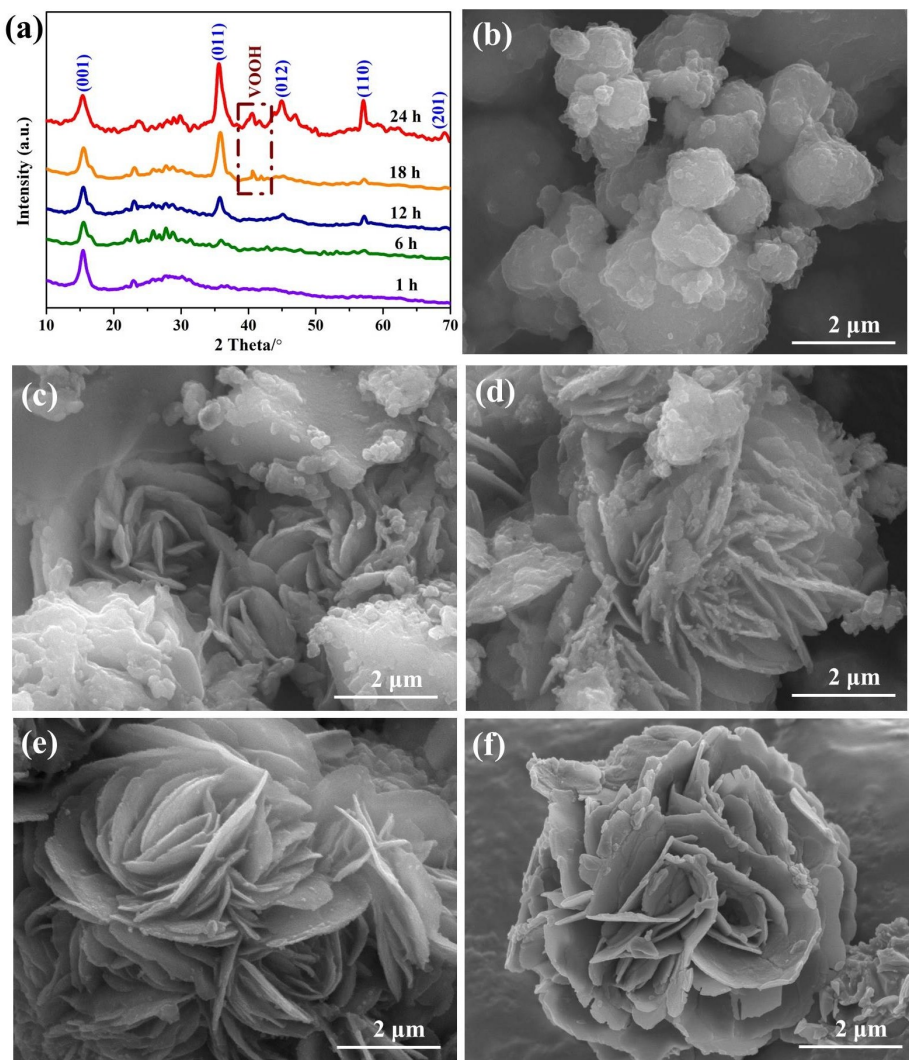


Fig. S7 (a) XRD patterns, and (b ~ f) SEM images of the products prepared at 1, 6, 12, 18 and 24 h, respectively.

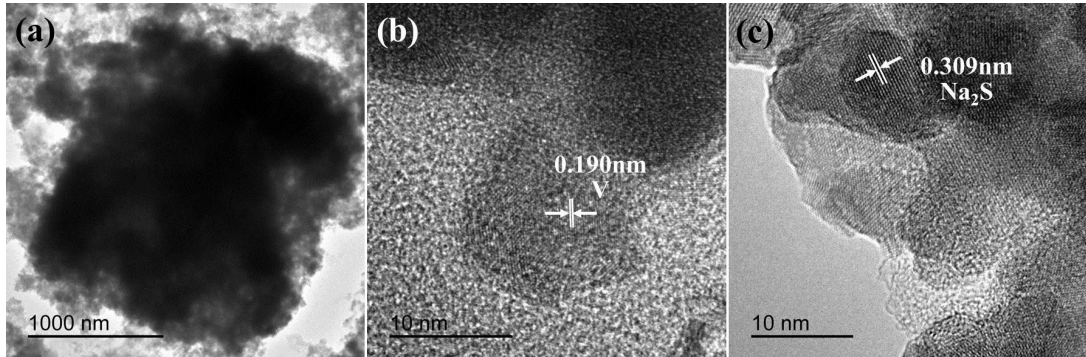


Fig. S8 TEM and HRTEM images of $c\text{-VS}_2@\text{VOOH}$ electrode materials after discharging to 0.05 V at 0.05 Ag^{-1} .

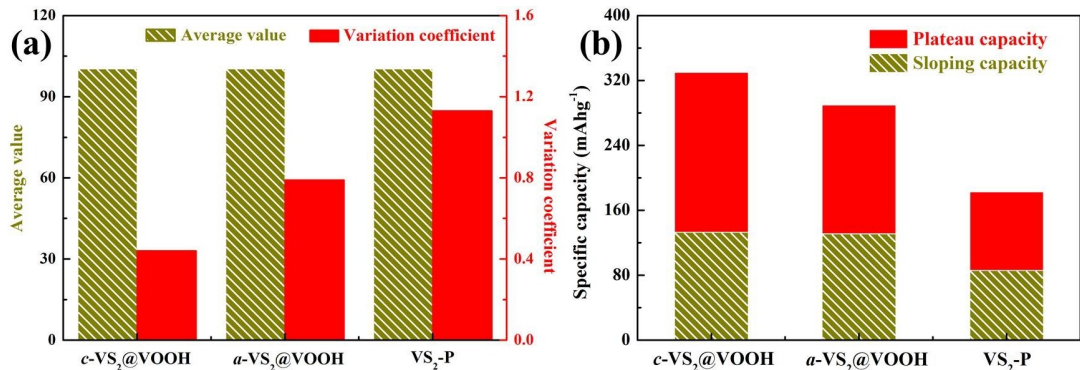


Fig. S9 (a) Average values and variation coefficients of the CEs derived from Fig. 8(b) and (b) plateau capacities and sloping capacities of the charge profiles in Fig. 8(c).

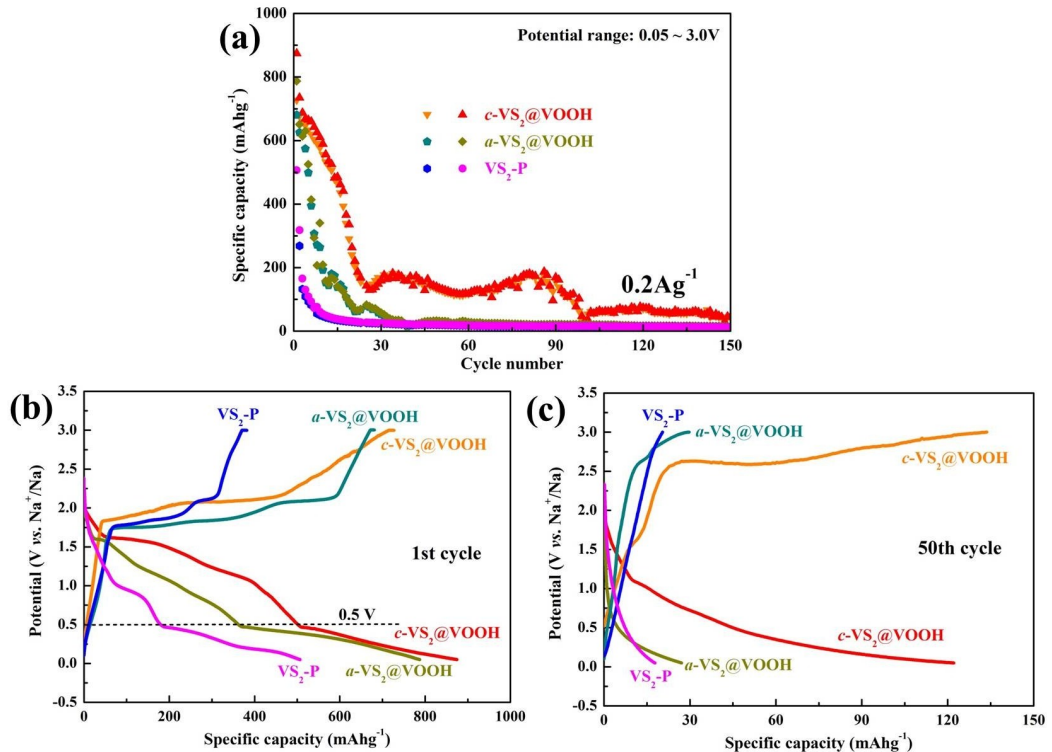


Fig. S10 (a) Cycling performances at the potential range of 0.05 ~ 3.00 V and corresponding to charge/discharge profiles after (b) 1 cycle and (c) 50 cycles for *c*-VS₂@VOOH, *a*-VS₂@VOOH and VS₂-P.

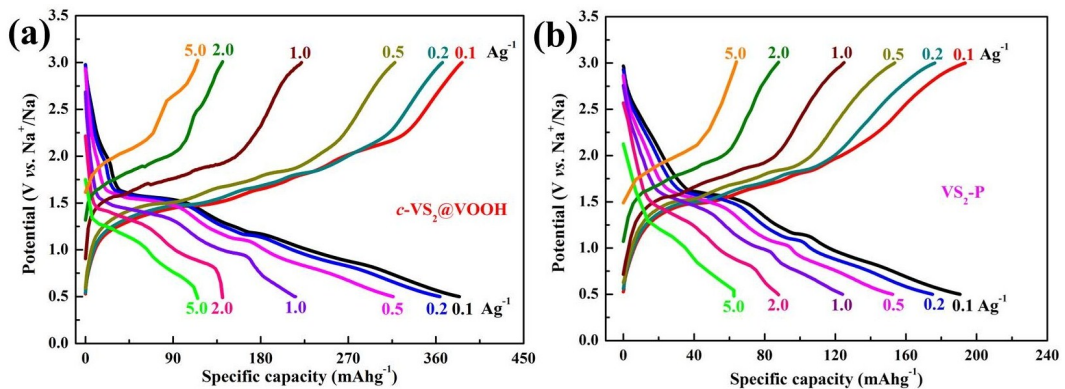


Fig. S11 Charge/discharge profiles of (a) *c*-VS₂@VOOH and (b) VS₂-P at various current densities from 0.1 to 5.0 Ag⁻¹.

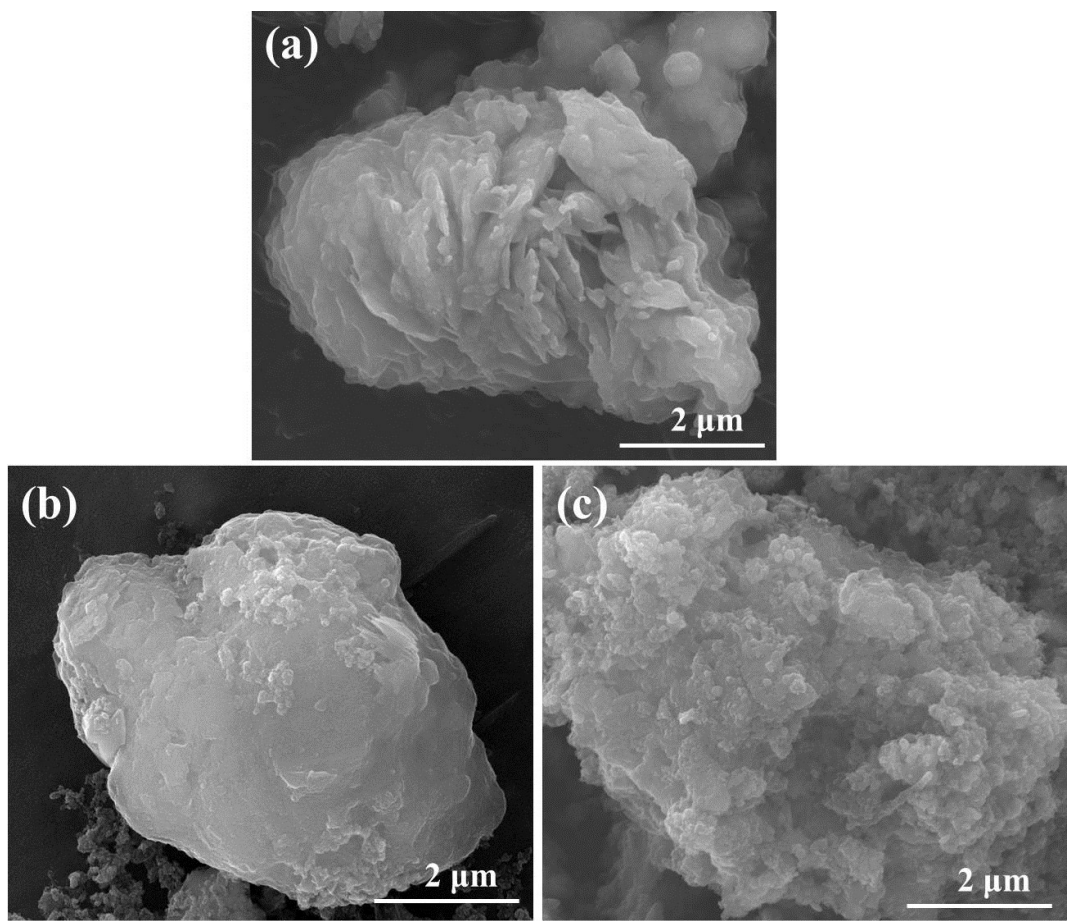


Fig. S12 SEM images of (a) *c*-VS₂@VOOH, (b) *a*-VS₂@VOOH and (c) VS₂-P electrode materials at 0.2 Ag⁻¹ after 150 cycles.

Table S1 Electrochemical performance comparison of the as-prepared *c*-VS₂@VOOH-based with other V-based and TMDs-based anode materials of SIBs.

Materials	Current density, A g ⁻¹	Cycling capacity, mAhg ⁻¹ , (cycle number, n)	Rate capacity, mAhg ⁻¹ , (Current density, A g ⁻¹)	Cut-off voltage (V)	Active material loading, mg·cm ⁻²	Electrode composition	Ref
<i>c</i> -VS ₂ @VOOH	0.2	330(150)	424(0.1), 404(0.2), 356(0.5), 224(1.0), 140(2.0), 113(5.0)	0.5~3.0	0.6~1.0	8:1:1	This work
VS ₂	0.2	245(100)	252(0.1), 211(0.5), 201(1.0), 196(2.0), 203(5.0)	0.4~2.2	0.84~1.05	7:2:1	5
ce-VS ₂	1.0	109(100)	----	0.01~3.0	~1.0	7:2:1	2
VS ₂ @Na ₂ Ti ₂ O ₅	0.2	203(50)	233(0.1), 210(0.4), 161(1.0), 124(2.0), 75(4.0)	0.01~3.0	1.0~1.5	----	6
VS ₄ /rGO	0.5	149(100)	341(0.1), 267(0.3), 220(0.5), 192(0.8)	0.01~2.2	0.84~1.05	7:2:1	7
ce-V ₅ S ₈ -C	1.0	496(500)	682(0.1), 643(0.2), 616(0.5), 584(1.0), 485(2.0), 389(5.0), 437(0.05), 375(0.1),	0.01~3.0	~1.0	7:2:1	2
VSe ₂ /C	0.1	467(50)	326(0.2), 309(0.5), 263(1.0), 132(2.0) 200(0.04), 185(0.08),	0~3.0	----	8:1:1	8
V ₂ O ₅	0.04	177(100)	157(0.16), 130(0.32), 122(0.64)	1.0~4.0	~0.88mg	8:1:1	9

VO ₂ /rGO	0.4	123(200)	196(0.04), 178(0.08), 160(0.16), 134(0.4), 108(0.8)	0.25~3.0	----	8:1:1	¹⁰
FeV ₂ S ₄	0.075	529(10)	548(0.075), 480(0.15), 372(0.375)	0~3.0	~3.0	8:1:1	¹¹
MoS ₂	0.32	234 (100)	498(0.04), 441(0.08), 409(0.16), 305(0.32)	0.01~3.0	~0.84	7:2:1	¹²
FeS ₂	0.2	256(60)	202(1.0)	0.8~3.0	----	8:1:0.4:0.6	¹³
WS ₂ NWs	0.5	362(500)	415(0.2), 370(0.5), 330(1.0)	0.5~3.0	----	7.5:1.5:1	¹⁴
ce-NbS ₂	0.5	157(100)	205(0.1), 185(0.2), 170(0.5), 137(1.0), 106(2.0), 93(5.0)	0.01~3.0	~0.7	7:2:1	¹⁵
NiS ₂ - GNs	0.1	313(200)	375(0.08), 325(0.16), 278(0.4), 221(0.8), 168 (1.6)	0.01~3.0	----	7:2:1	¹⁶
TiS ₂	0.48	141(300)	189(0.048), 180(0.12), 148(0.48), 123(1.2), 100(2.4)	1.0~3.0	----	8:1:1	¹⁷
CoS ₂ - MWCNT	0.1	568(100)	727(0.1), 687(0.2), 621(0.4), 550(0.8)	1.0~2.9	----	8:1:1	¹⁸

The list of electrode composition ratio contains the active material, the conductive material and the binder.

----: The relevant data is not mentioned in the article.

Table S2 Resistance values simulated from modeling the experimental impedance (Fig. 10) using the equivalent circuit shown in the inset in the bottom right of Fig. 10(a).

Sample	R_s (Ω)	R_f+R_{ct} (Ω)	Z_w ($\Omega \cdot S^{1/2}$)
<i>c</i> -VS ₂ @VOOH	11.7	7.9	42
<i>a</i> -VS ₂ @VOOH	22.4	22.0	87
VS ₂ -P	54.0	86.7	123

R_s is the electrolyte resistance. R_f is the SEI film resistance. R_{ct} is the charge-transfer resistance from electrolyte to active materials. Z_w is the Warburg resistance.

References

1. C. S. Rout, B.-H. Kim, X. Xu, J. Yang, H. Y. Jeong, D. Odkhuu, N. Park, J. Cho and H. S. Shin, *J. Am. Chem. Soc.*, 2013, **135**, 8720-8725.
2. C. Yang, X. Ou, X. Xiong, F. Zheng, R. Hu, Y. Chen, M. Liua and K. Huang, *Energy Environ. Sci.*, 2017, **10**, 107-113.
3. V. O. Koroteev, L. G. Bulusheva, I. P. Asanov, E. V. Shlyakhova, D. V. Vyalikh and A. V. Okotrub, *J. Phys. Chem. C*, 2011, **115**, 21199-21204.
4. L. Zhao, X. Li, C. Hao and C. L. Raston, *Appl. Catal. B-Environ.*, 2012, **117-118**, 339-345.
5. R. Sun, Q. Wei, J. Sheng, C. Shi, Q. An, S. Liu and L. Mai, *Nano Energy*, 2017, **35**, 396-404.
6. J.-Y. Liao and A. Manthiram, *Nano Energy*, 2015, **18**, 20-27.
7. R. Sun, Q. Wei, Q. Li, W. Luo, Q. An, J. Sheng, D. Wang, W. Chen and L. Mai, *ACS Appl. Mater. Interfaces*, 2015, **7**, 20902-20908.
8. X. Yang and Z. Zhang, *Mater. Lett.*, 2017, **189**, 152-155.
9. D. Su, S. Dou and G. Wang, *ChemSusChem*, 2015, **8**, 2877-2882.
10. G. He, L. Li and A. Manthiram, *J. Mater. Chem. A*, 2015, **3**, 14750-14758.
11. M. Krengel, P. Adelhelm, F. Kleinc and W. Bensch, *Chem. Commun.*, 2015, **70**, 13500-13503.
12. D. Su, S. Dou and G. Wang, *Adv. Energy Mater.*, 2015, **5**, 1401205.
13. Z. Hu, Z. Zhu, F. Cheng, K. Zhang, J. Wang, C. Chen and J. Chen, *Energy Environ. Sci.*, 2015, **8**, 1309-1316.

14. Y. Liu, N. Zhang, Hongyan Kang, M. Shang, L. Jiao and J. Chen, *Chem.-Eur. J.*, 2015, **21**, 11878-11884.
15. X. Ou, X. Xiong, F. Zheng, C. Yang, Z. Lin, R. Hu, C. Jin, Y. Chen and M. Liu, *J. Power Sources*, 2016, **325**, 410-416.
16. T. Wang, P. Hu, C. Zhang, H. Du, Z. Zhang, X. Wang, S. Chen, J. Xiong and G. Cui, *ACS Appl. Mater. Interfaces*, 2016, **8**, 7811-7817.
17. Y. Liu, H. Wang, L. Cheng, N. Han, F. Zhao, P. Li, C. Jin and Y. Li, *Nano Energy*, 2016, **20**, 168-175.
18. Z. Shadike, M.-H. Cao, F. Ding, L. Sangb and Z.-W. Fu, *Chem. Commun.*, 2015, **52**, 10486-10489.